Journal of Applied Polymer Science

Investigation of adsorption behaviors of Cu(II), Pb(II), and Cd(II) from water onto the high molecular weight poly (arylene ether sulfone) with pendant carboxyl groups

Xinghua Wu, Dazhi Wang, Shaoyin Zhang, Weijie Cai, Yuxin Yin
Department of Applied Chemistry, Faculty of Light Industry and Chemical Engineering, Dalian Polytechnic University, Dalian 116034, China
Correspondence to: S. Zhang (E-mail: zhangsy@dlpu.edu.cn)

ABSTRACT: Three types of high molecular weight polyarylether adsorbents with different molar ratios of carboxyl and phenylene were designed and synthesized through direct polycondensation in mixture solvents. The as-prepared polymers were characterized by FTIR, ^{1}H-NMR, TGA, DSC, SEM, EDS, and GPC in order to study the regularity of polymeric adsorption/thermostability performances. Because of the highest molar ratio of carboxyl and phenylene, PAES-C-Na presented the highest adsorption capacity of Cu^{2+} compared to PAESK-C-Na and PAES; therefore, PAES-C-Na was opted to study the impacts of adsorbent dosage, pH, contact time, and initial concentration on the adsorption of Pb^{2+} and Cd^{2+}. Moreover, a kinetic analysis revealed that the adsorption process followed pseudo-second-order model, while the thermodynamic experimental data properly fitted with the Freundlich model. The multi-component competitive adsorption capacity followed the order $Pb^{2+} > Cu^{2+} > Cd^{2+}$. Additionally, the regeneration tests indicated that PAES-C-Na still possessed the excellent adsorption capacity after several recycles. © 2015 Wiley Periodicals, Inc. J. Appl. Polym. Sci. **2015**, *132*, 41984.

KEYWORDS: adsorption; applications; functionalization of polymers; kinetics; properties and characterization

Received 15 June 2014; accepted 10 January 2015
DOI: 10.1002/app.41984

INTRODUCTION

The removal of the heavy metal ions has been under increased scrutiny consideration that their toxicity and nonbiodegradability result in the serious environmental problems.[1] Various techniques such as chemical precipitation, solvent extraction, nanofiltration, membrane separation, and adsorption have been utilized to remove heavy metal ions from wastewater.[2–6] Among them, adsorption was regarded as one of the most promising methods for heavy metal ions removal due to its high efficiency, simple operation, and environmental friendliness.[7] Up to date, a variety of adsorbents including activated carbon, modified silica gel, multi-walled carbon nanotubes (MWCNTs), polymers, bio-derived materials, and sorption resins have been reported as the suitable candidates for heavy metals ions elimination.[8–13] It was demonstrated that polymeric adsorbents exhibited the higher adsorption capacity, compared with other adsorbents due to its strong mechanical property, excellent thermal stability, and the intense interaction with metal ions.[14]

It was well-accepted that the interaction between heavy metal ions and the functional groups such as carboxyl, amide, sulfonyl or imidazolyl in the polymeric structure played a key role in the adsorption capacity of the as-prepared polymeric adsorbents.[15–17] In addition to the remarkable mechanical property and stability, polymeric adsorbents with high molecular weight might form more pores and holes.[18] Thanks to all these merits, the high molecular weight polyarylether was functionalized to meet with the severe application conditions.[7]

Based on the above consideration and molecular design, three types of high molecular weigh polyarylether adsorbents with various molar ratios of carboxyl and phenylene were successfully synthesized in this work. First, poly (arylene ether sulfone) without carboxylic groups (PAES) was prepared with 4,4′-dichlorodiphenylsulfone (DCDPS) and bisphenol A (BPA). Another two polymers containing carboxylic groups (poly (arylene ether sulfone) (PAES-C) and poly (arylene ether sulfone ketone) (PAESK-C)) were achieved with dichloro-monomer (DCDPS, 1-(p-chlorobenzoyl)-3-(p-chlorobenzen esulfonyl) benzene) and bisphenol-monomer (4,4′-bis(4-hydroxyphenyl)-pentanoic acid (DPA)). The use of DPA sourced from the renewable biomass might efficiently resolve the dwindling resources and environmental pollution problems caused by the

Additional Supporting Information may be found in the online version of this article.

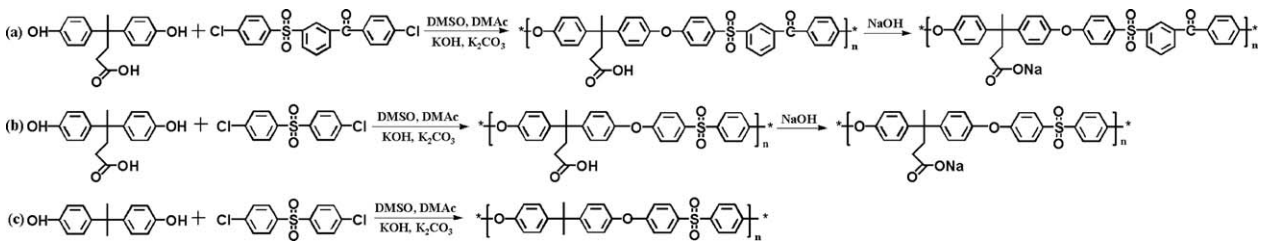

Scheme 1. Syntheses of polymers: (a) PAESK-C-Na, (b) PAES-C-Na and (c) PAES.

conventional technology for polymeric materials production.[19,20] At present, DPA and its derivatives have been extensively applied in polymers synthesis, but little focused on the heavy metal ions removal such as Cu^{2+}, Pb^{2+}, and Cd^{2+} from wastewater with the as-prepared polymers.[21–23]

Furthermore, this work aimed to investigate the adsorption abilities of Cu^{2+} onto polymers containing sodium salt (poly (arylene ether sulfone) with sodium carboxylate groups (PAES-C-Na), poly (arylene ether sulfone ketone) with sodium carboxylate groups (PAESK-C-Na)), and PAES which contains various molar ratios of carboxyl and phenylene. PAES-C-Na and PAESK-C-Na were obtained from the as-prepared PAES-C and PAESK-C with NaOH, respectively. PAES-C-Na with the best adsorption capacity of Cu^{2+} was selected to further study the removal of other ions (Pb^{2+}, Cd^{2+}) from wastewater and elucidated the adsorption isotherms and kinetic model of Cu^{2+}, Pb^{2+}, and Cd^{2+}. FTIR, SEM, EDS, GPC, and BET were used to characterize the as-prepared polymers.

EXPERIMENTAL

Materials

DPA, BPA, DCDPS, anhydrous potassium carbonate (K_2CO_3) and potassium hydroxide (KOH) were purchased from the Sinopharm Chemical Reagent (China). 1-(p-chlorobenzoyl)-3-(p-chlorobenzen esulfonyl) benzene contained carbonyl and sulfonyl was synthesized in our group. Prior to the preparation, DCDPS, 1-(p-chlorobenzoyl)-3-(p-chlorobenzen esulfonyl) benzene, BPA, and DPA were vacuum dried at 100°C for 24 h, while K_2CO_3 was pretreated at 150°C for 24 h. *N,N′*-dimethylacetamide (DMAC) and dimethyl sulfoxide (DMSO) were purchased from the Kermel company (China) and purified by the distillation under the low pressure over calcium hydride and stored in a vacuum chamber. Other solvents were used as received. All chemicals used in this article were of A.R. grade. Stock solution (1 mg/mL) of Cu^{2+}, Pb^{2+}, and Cd^{2+} were prepared by dissolving the appropriate amounts of nitrate salt of metal ($Cu(NO_3)_2{\cdot}2H_2O$, $Pb(NO_3)_2$ and $Cd(NO_3)_2$) in deionized water, respectively. The experimental solutions of desired concentration were prepared by successive dilution of stock solution.

Synthesis of the Polymers

Polymerization was conducted in the liquid phase with continuous nitrogen flow using a 100 mL round bottomed flask equipped with a nitrogen inlet, a stir bar, and a Dean-Stark trap. The detailed polymerization procedure of PAES-C was described as followed: A mixture of bisphenol-monomer DPA (0.005 mol), K_2CO_3 (0.0075 mol), KOH (0.0025 mol), toluene (15 mL), DMAC (10 mL), and DMSO (10 mL) (20 wt % solids concentration of DMAC and DMSO mixture), was stirred at room temperature for 2 h and then heated to 150°C under refluxing for 3 h to remove the azeotropic mixture of water and toluene. After naturally cooled to room temperature, dichloro-monomer DCDPS (0.005 mol) was added and then the mixture was heated at 150°C for 2–3 h. The mixture was further heated to 175°C, until the solution became viscous. After cooling down to room temperature the solution was diluted in 90 mL of tetrahydrofunan (THF)/HCl mixture (the volume ratio of 4/5). The white precipitate appeared once the solution was poured into 500 mL deionized water. After washed with hot deionized water and ethanol, the PAES-C was dried under vacuum at 100°C for 24 h. Similarly, another two polymers (PAESK-C, PAES) were prepared by the bisphenol-monomer (DPA, BPA) and the dichloro-monomer (1-(p-chlorobenzoyl)-3-(p-chlorobenzen esulfonyl) benzene, DCDPS) with the above polymerization procedures. To obtain PAES-C-Na and PAESK-C-Na, the as-prepared PAES-C and PAESK-C were put into 200 mL NaOH solution (0.1 mol/L) with continuous stirring for 5–6 h, followed by filtering and vacuum drying at 100°C for 24 h. The synthetic processes of polymers were briefly presented in Scheme 1.

Preparation of Polymer Membranes

Polymer samples (1 g) were dissolved into NMP (10 mL) and then cast onto the glass plate. After drying at 60°C for 10 min, the membranes were further cured at 100°C for 24 h under vacuum. Subsequently, the glass plate was immersed into 500 mL deionized water for 5 h to achieve membranes. The obtained solid membranes were dried at 100°C for 24 h under vacuum, showing flexible and transparent-to-gray in color, with the thickness ranging from 30 to 50 μm.

Polymer Characterizations

Fourier transform infrared (FTIR) spectroscopy analysis was performed in the region of 4000-500 cm^{-1} (Perkin Elmer, USA).

^{1}H-NMR (400 MHz) spectra of the polymers were recorded using a Varian INOVA spectrometer with dimethylsulfoxide-d_6 (DMSO-d_6) as a solvent.

The thermal degradation processes were investigated using a thermogravimetric analyzer (TGA, TA Instruments Q50, USA). The samples were dried at 150°C for 24 h in a vacuum oven prior to the measurement. The TGA measurements were carried out under a nitrogen atmosphere at a heating rate of 10°C/min ranging from 20 to 700°C.

Differential scanning calorimetry (DSC) measurements were undertaken at differential scanning calorimeter (DSC 2000, TA Instruments) equipped with a cooling unit. The samples were also dried at 100°C for 24 h in a vacuum oven prior to the measurement.

Table I. Adsorption Experimental Conditions for Metal Ions on PAES-C-Na

Experiments	Initial metal ions concentration (mg/L)	PH	Adsorbbent dosage (g/L)	Contact time (h)
Effect of adsorbent dosage	10	5	0.17, 0.2, 0.25, 0.33, 0.5, 1	15
Effect of pH	10	1, 2, 3, 4, 5, 6, 7	0.25	15
Effect of contact time	10	5	0.25	1, 1.5, 2, 2.5, 3, 3.5, 4, 4.5, 5, 6, 7, 8, 9, 10,11,12,13,14,15
Effect of initial metal ions concentration	3.5, 5, 10, 20, 30, 40, 50	5	0.25	15

A DSC thermogram was recorded under ultra high purity nitrogen at a heating rate of 10°C/min ranging from 25 to 300°C.

A wide-angle X-ray diffraction ranging from 4 to 80° was conducted to determine the polymers' physicochemical property using Cu-Kα X-radiation at room temperature (D/Max-3B X-ray diffractometer, Japan).

Relative molecular weight was obtained using Gel permeation chromatography (GPC) (Waters® Corporation, USA) equipped with a refractive index detector(Waters® 2414). Degassed THF was used as eluent at a flow rate of 0.6 mL/min towards Styrogel® column. A set of monodisperse polystyrene standards covering the range of 10^3-10^6 were used for the molecular weight calibration. Samples were dissolved into THF and filtered over a 0.45-μm filter membrane before injected into the GPC.

Flame atomic absorption spectrometry (FAAS) (HG-9602) equipped with a flame burner was employed to determine the absorbance of metal ions. As to the determination of Cu^{2+}, Pb^{2+}, and Cd^{2+} ions, corresponding lamp wavelength was set at 324.7 nm, 283.3 nm, and 228.8 nm, respectively, and all lamp currents were 3 mA.

The microstructure, morphology and elemental composition of the polymers were investigated using a scanning electron microscope (SEM, JEOL JSM-6380) along with Energy dispersive X-ray spectroscopy (EDS).

Brunauer-Emmett-Teller (BET) specific surface area and pore volume were measured from N_2 adsorption-desorption isotherms at -196°C with a model NOVA-2200E automated gas sorption system (Quantachrome, USA).

The mechanical property of the membranes was measured at a rate of 10 mm min^{-1} using an electronic universal testing machine (UTM model RGT-5, Reger Instrument, Shenzhen). The samples had the following dimensions: 15 mm length × 4 mm width. The tests were conducted three times.

Optimal Adsorbent Selection

The adsorption abilities of Cu^{2+} onto PAESK-C-Na, PAES-C-Na and PAES were performed by shaking 0.01 g adsorbents with 40 mL Cu^{2+} (3.5 mg/L) with the pH values ranging from 1.0 to 7.0 at 200 rpm for 15 h at 30 ± 2°C. The suspension was filtered and the metal ions concentration in the filtrate was measured using the FAAS.

Adsorption of Various Metal Ions on PAES-C-Na

In a typical procedure, the batch adsorption studies of Cu^{2+}, Pb^{2+}, and Cd^{2+} onto the PAES-C-Na were performed in different concentrated Cu^{2+}, Pb^{2+}, and Cd^{2+} solutions, and different dosage of the PAES-C-Na within the pH values ranging from 1.0 to 7.0 under shaking at 200 rpm for 0.5-15 h at 30 ± 2°C. The detailed experiment parameters were shown in Table I.

The standard deviations calculated from each experiment were less than 5.0% in all cases. Both the adsorption percentage of metal ions and the adsorption capacity were calculated in terms of following equations:

$$\text{Adsorption}(\%) = \frac{C_0 - C_e}{C_0} \times 100 \quad (1)$$

$$q_e = \frac{(C_0 - C_e)V}{m} \quad (2)$$

where C_0 and C_e represent initial and equilibrium metal ion concentrations (mg/L), respectively. V is the volume of metal ion (mL), m is the amount of adsorbent (mg), and q_e means the equilibrium adsorption capacity of metal ions (mg/g).[7]

Competitive Adsorption of Metal Ions on PAES-C-Na

Competitive adsorption of Cu^{2+}, Pb^{2+}, and Cd^{2+} with the fixed concentration (10 mg/L) was conducted by shaking 0.01 g adsorbents with 40 mL solution (pH = 5.0) at 200 rpm for 15 h at 30 ± 2°C. The suspensions were filtered and the metal ions concentration in the solutions was measured using the FAAS.

Regeneration of PAES-C-Na

To recycle PAES-C-Na, the samples loaded with heavy metal ions were added into HCl solution (0.1 mol/L) with stirring for 5 h and then washed with deionized water until the neutral. During this process, the adsorbed metal ions were decomposed and subsequently released from solid adsorbents into desorption medium.[7] After further stirring for 5 h in NaOH solution (0.1 mol/L), PAES-C-Na were obtained by filtration and vacuum dried at 100°C for 24 h.

RESULTS AND DISCUSSION

Structures of Polymers

All polymers were confirmed by ^{1}H-NMR spectra (Figure 1) for their chemical structures. For PAES-C spectrum, the peaks

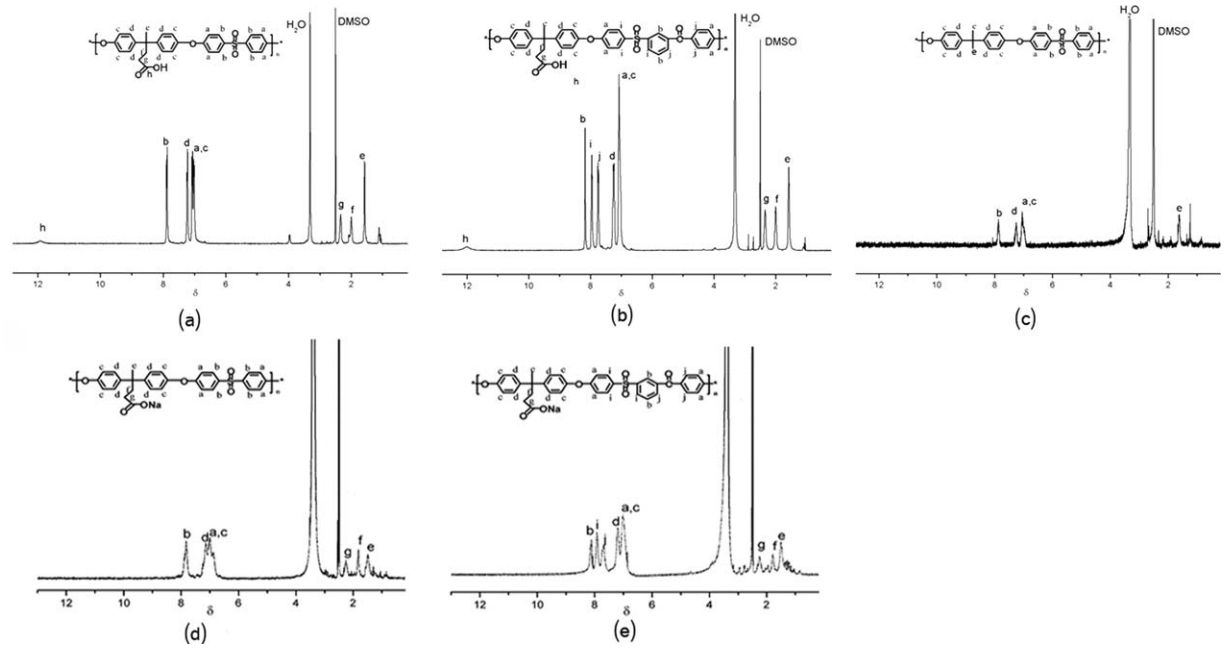

Figure 1. ^{1}H-NMR spectra of polymers: (a) PAES-C, (b) PAESK-C, (c) PAES, (d) PAES-C-Na, and (e) PAESK-C-Na.

at 1.5–2.5 ppm are due to the vibration of aliphatic protons in polymeric chain, and the peaks observed in the region of 6.5–8.5 ppm corresponds to the aromatic protons. Compared with the spectrum of PAES, a new peak appears at 12 ppm, confirming that the carboxylic group was successfully incorporated into PAES-C structure.[22] As to PAESK-C spectrum, the aromatic protons peaks centering at 7.74, 7.95, and 8.17 ppm are observed due to the effect of the carbonyl groups in molecular main-chain. As shown in Figure 1(d,e), the absence of the peak at 12 ppm suggested the formation of sodium salt of polymers (PAES-C-Na and PAESK-C-Na).

The IR spectra of polymers were presented in Figure 2(a). For PAES-C, the peak at 3430 cm^{-1} is the characteristic peak of hydroxyl in carboxylic groups,[24] representing the existence of the carboxyl group (–COOH) in polymer. The peaks at 1143 and 1294 cm^{-1} illustrate the asymmetric and symmetric stretching vibration of O═S═O group, while the absorption bands around at 690 and 1737 cm^{-1} are attributed to the stretching vibration of C—S and C═O in carboxylic groups, respectively.[21] Moreover, the bands at 1238 and 1013 cm^{-1} are assigned to the asymmetric and symmetric stretching vibration of Ph—O—Ph group. Compared with the PAES-C spectrum, the adsorption band at 1662 cm^{-1} could be ascribed to the stretching vibration of C═O group in the main-chain of PAESK-C. However, the bands around at 1737 cm^{-1} (C═O) and 3430 cm^{-1} (—OH) are not observed because of the absence of —COOH groups in the structure of PAES. As shown in Figure 2(b), the formation of the sodium salt of polymers[25] resulted in the intensity decline

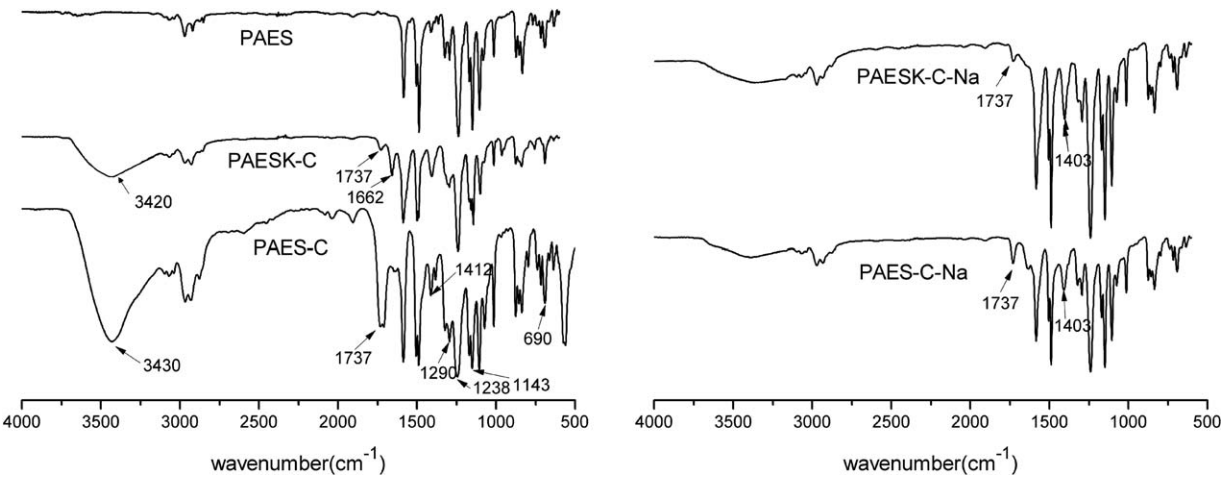

Figure 2. FTIR spectroscopes of polymers: (a) PAES-C, PAESK-C and PAES(b) PAES-C-Na, and PAESK-C-Na.

Table II. GPC Data of Polymers, as Calculated towards Polystyrene Standards

Dist name	M_n	M_w	M_p	M_z	M_{z+1}	Polydispersity
PAESK-C	16,579	36,425	40,341	54,442	66,733	2.19
PAES-C	54,614	128,482	94,737	234,585	331,183	2.33
PAES	21,205	43,808	59,350	59,439	69,479	2.07

of the peak at about 1737 cm^{-1} and the change of the peak intensity at about 1403 cm^{-1}. In line with the ^{1}H-NMR spectra, the FTIR results clearly indicated the successful synthesis of the targeted polymers.

Molecular Weight of Polymers

PAES-C-Na and PAESK-C-Na with the highly molecular weight were prepared by direct polycondensation in mixed solvent (DMSO/DMAc). During the polymeric synthesis process, the decline of solubility together with the chain growing might lead to the two-phase separation in the single solvent system.[26] Therefore, the mixture solvent ($V_{DMSO}/V_{DMAc} = 1/1$) with the better solubility of polymers could efficiently weaken the degree of two-phase separation. As presented in Table II, the obtained polymers possessed the higher molecular weight and the more rational distribution, compared with the reported polymer,[27] which was helpful to improve the thermal stability and mechanical property of the polymer. Hence, it also supplied the possibility to form pores and holes in order to enhance the adsorption capacity.[18]

Mechanical Properties of Polymers

The membranes obtained from PAES-C-Na, PAESK-C-Na, and PAES exhibited the tensile strength of 87.34 MPa, 76.38 MPa, and 83.96 MPa, respectively. It illustrated that the larger molecular weight resulted in the stronger mechanical property. Compared with PAES sample, PAES-C-Na polymer presented the stronger tensile strength because of its more flexible carboxyl groups.

Morphologies of Polymers

Only a broad peak was observed in the XRD patterns (Supporting Information Figure S1 (ESI)). It indicated the amorphous structure of the polymers, which were in concert with the DSC results.

The surface morphology of polymers was investigated by SEM technique (Supporting Information Figure S2 (ESI)). The roughly uniform pores with the size about 5-20 μm (PAES-C-Na) and 10-20 μm (PAESK-C-Na) respectively are observed. The pore structure could efficiently avoid mass transfer limitation and diffusion resistance during the adsorption process in comparison with the PAES sample with smaller pores.[18] Figure 3 presented the spectra for PAES-C-Na loaded with heavy metal ions, where Cu^{2+} was selected as model ions. The surface morphology of PAES-C-Na remained unchanged before and after Cu^{2+} sorption.

Based on the BET results of polymers, PAES-C-Na presented an adequate surface area (21.832 m^2/g) and pore volume (0.032 cc/g); Nevertheless, both PAESK-C-Na and PAES exhibited a smaller surface area (12.879 m^2/g, 8.684 m^2/g) and pore volume (0.012 cc/g, 0.009 cc/g), respectively. The highest surface area and pore volume might improve the adsorption capacity of PAES-C-Na for the metal ions from wastewater.[29]

Thermal Analysis of Polymers

The thermal stability of polymers was investigated by TGA measurement. A single step degradation peak at around 380°C

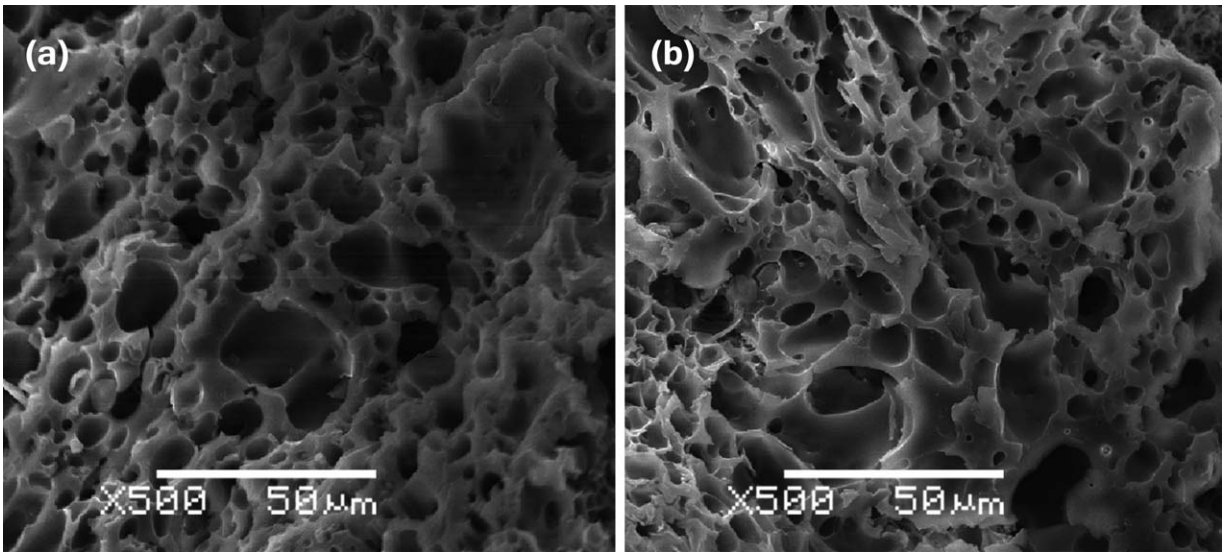

Figure 3. SEM images of PAES-C-Na: (a) before Cu^{2+} adsorption and (b) after Cu^{2+} adsorption.

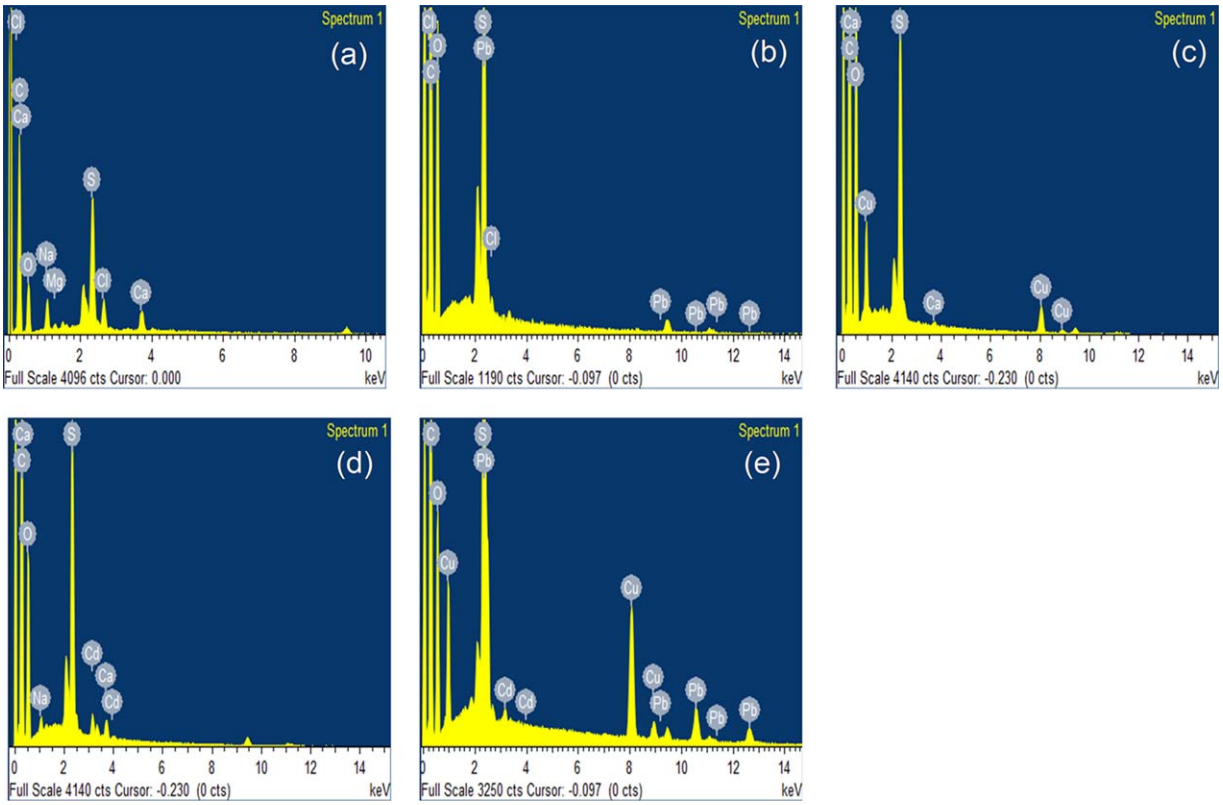

Figure 4. EDS spectra of PAES-C-Na: (a) before adsorption, (b) after Cu^{2+} adsorption, (c) after Pb^{2+} adsorption, (d) after Cd^{2+} adsorption and (e) after competitive adsorption. [Color figure can be viewed in the online issue, which is available at wileyonlinelibrary.com.]

(PAES-C), 392°C (PAESK-C), and 461°C (PAES) within a 5% weight loss were screened in Supporting Information Figure S3 (ESI), which probably were related to the degradation of polymeric chain. Obviously, the polymers with the higher molar ratio of carboxyl and phenylene showed the lower degradation temperature, that is, the presence of carboxyl groups decreased the degradation temperature.

The glass transition temperature (T_g) of polymers were measured by DSC technique. As shown in Supporting Information Figure S4 (ESI), it illustrated that the midpoints of the heat capacity step change were ca. 177°C (PAESK-C), ca. 165°C (PAES-C), and ca. 170°C (PAES), respectively. The presence of carboxylic acid groups into PAES-C branched-chain reduced the regularity and crystallinity of molecular chain,[12] compared with PAES. And, PAESK-C possessed structurally more rigid groups than PAES-C. Hence, T_g followed the order PAESK-C-Na > PAES > PAES-C-Na. Additionally, no obvious endothermic or exothermic peaks were observed except one peak corresponding to the glass transition of polymer, which illustrated that no cross-linked side-reaction occurred.[30] This demonstrated the as-prepared polymers exhibited the well thermal stability.

Comparison of Adsorption Performances Between PAES-C and PAES-C-Na

The result showed that the adsorption efficiency of PAES-C-Na (97%) was much higher than the value of PAES-C (10.6%) probably due to electrostatic attraction[31]—the lone-pair electrons in the oxygen atom may be shared by the oxygen atom and Cu^{2+}. PAES-C-Na possessed more lone-pair electrons causing stronger electrostatic attraction in aqueous solution, compared to PAES-C. In consequence, the sodium salt of polymer was selected to further investigate the influence of various reaction parameters.

Evaluation of Different Adsorption Materials

PH Effects of Cu^{2+} on PAES-C-Na, PAESK-C-Na and PAES. The pH value of solution has been regarded as the most important controlling factors in the heavy metal elimination process. It strongly affected the surface charge of the adsorbent as well as the degree of ionization and speciation of the heavy metal in the solution.[32] The tests were conducted in the pH range (1.0-7.0), and the influence of pH on the adsorption capacity for Cu^{2+} was demonstrated in Supporting Information Figure S5 (ESI). For PAES-C-Na and PAESK-C-Na, no obvious difference of the adsorption capacity is observed at pH value below 3.0, and the adsorption percentage rapidly increases with further increasing pH value to 5.0, but then levels off (5.0-6.0). Because at lower pH values (1.0-3.0), the solution contains high concentration of H^+ ions, which had high mobility and then competed with the metal ions for active sites on the adsorbents.[23] Another reason may be ascribed to the fact that the extensive repulsion of metal ions and protonated carboxylic groups of the adsorbent surface weakened the ion-exchange interaction. With increasing pH values (3.0-6.0), the formation of ionized carboxylic groups created the strong electrostatic interaction with the metal ions, resulting in high uptake.

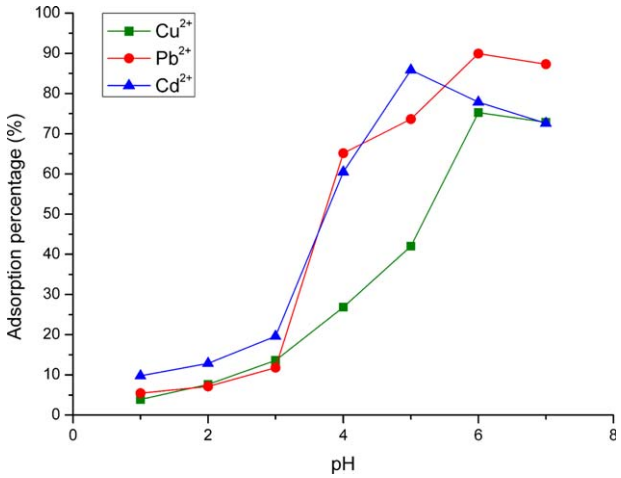

Figure 5. Effect of pH on the adsorption of Cu^{2+}, Pb^{2+}, and Cd^{2+} onto PAES-C-Na. [Color figure can be viewed in the online issue, which is available at wileyonlinelibrary.com.]

However, a slight decline of the adsorption performance upon rising pH from 6.0 to 7.0 was probably assigned to the formation of $Cu(OH)_2(s)$ at a pH value above 6.2.[1] An unobvious change of the adsorption capacity of Cu^{2+} on PAES was screened with increasing pH value due to no carboxylic functional groups in PAES. The difference in adsorption capacity of different adsorption materials could be explained on the basis of the difference of molar ratios between carboxyl and phenylene, namely, the adsorbents with the higher molar ratios (PAES-C-Na > PAESK-C-Na > PAES) had the larger adsorption capacities.

Adsorption Isotherms of Cu^{2+} on PAES-C-Na, PAESK-C-Na, and PAES. For better understanding the adsorption process, three adsorption isotherm models were investigated.[29] The linear isotherm (or Henry isotherm) [eq. (3)], Freundlich isotherm [eq. (4)] and the Langmuir isotherm [eq. (5)] were applied:

$$q_e = K_d \cdot C_e \tag{3}$$

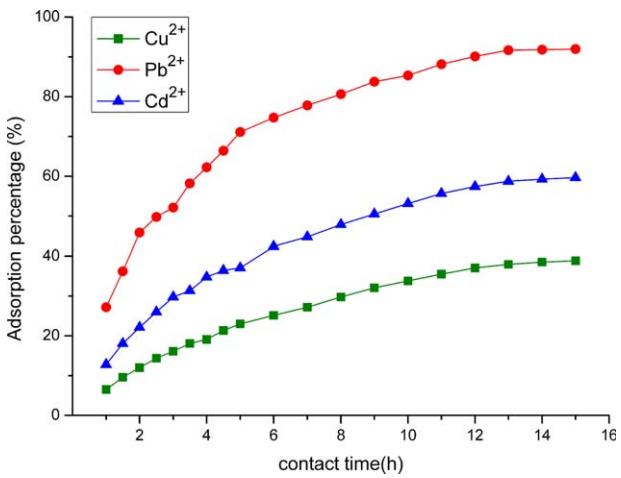

Figure 6. Effect of contact time on the adsorption of Cu^{2+}, Pb^{2+}, and Cd^{2+} onto PAES-C-Na. [Color figure can be viewed in the online issue, which is available at wileyonlinelibrary.com.]

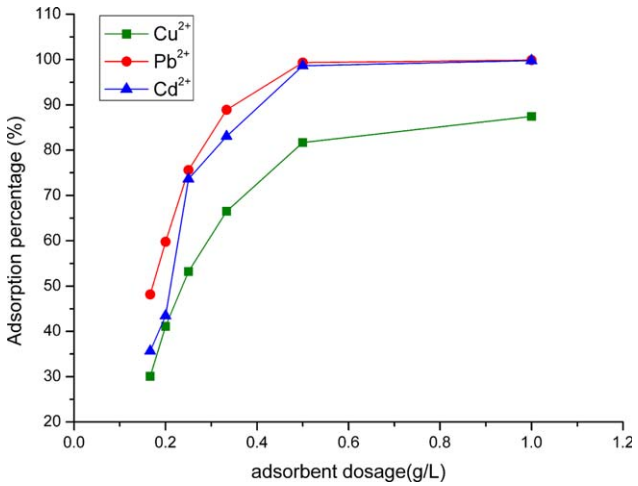

Figure 7. Effect of adsorbent dosage on the adsorption of Cu^{2+}, Pb^{2+}, and Cd^{2+} onto PAES-C-Na. [Color figure can be viewed in the online issue, which is available at wileyonlinelibrary.com.]

$$\log(q_e) = \log(K) + \frac{1}{n}\log(C_e) \tag{4}$$

$$\frac{C_e}{q_e} = \frac{1}{b \cdot q_m} + \frac{C_e}{q_m} \tag{5}$$

where K_d is the linear adsorption coefficient (L/g), K and n are Freundlich constants related to adsorption capacity (L/g) and adsorption intensity of adsorbents, q_m is a Langmuir parameter that expresses the maximum metal uptake (mg/g), b is the Langmuir constant related to the adsorption energy (L/mg), q_e is the Cu^{2+} adsorption density (mg/g) at equilibrium, and C_e is the equilibrium metal ion concentration in the solution (mg/L).

As presented in Supporting Information Supporting Information Figure S6 and Table S1 (ESI), the Freundlich isotherms model with a higher correlation coefficient made it as a suitable candidate to describe the adsorption equilibrium for the tested materials and the order of Cu^{2+} sorption capacity of PAES-C-Na, PAESK-C-Na, and PAES was as followed: PAES-C-

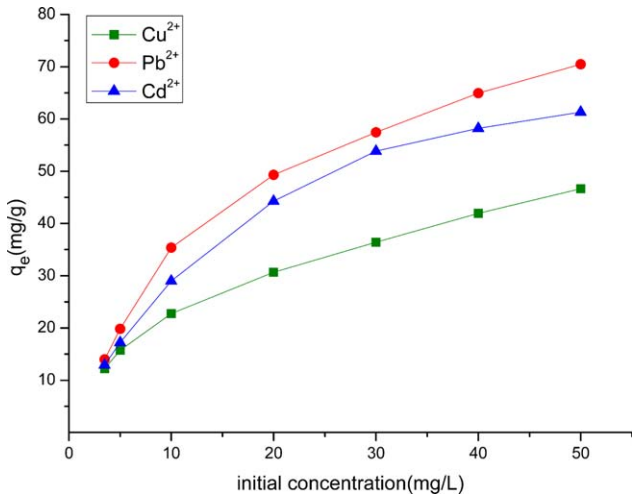

Figure 8. Effect of initial concentration on the adsorption of Cu^{2+}, Pb^{2+}, and Cd^{2+} onto PAES-C-Na. [Color figure can be viewed in the online issue, which is available at wileyonlinelibrary.com.]

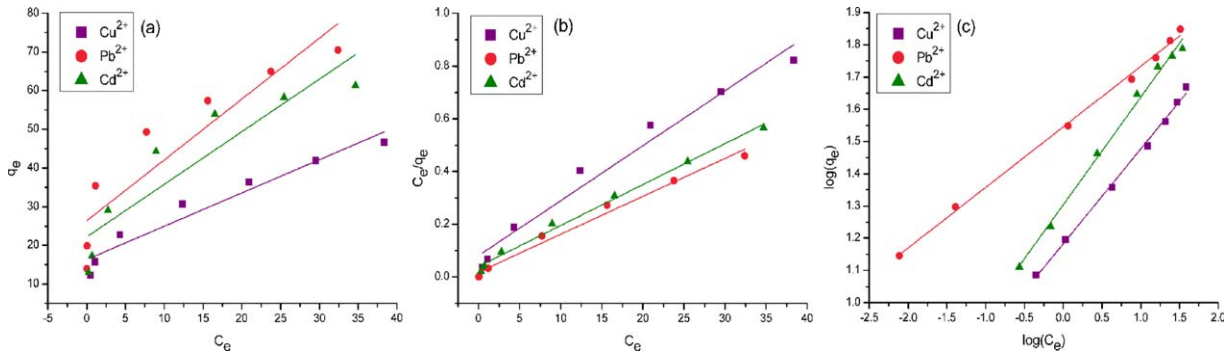

Figure 9. (a) Henry, (b) Langmuir, and (c) Freundlich adsorption isotherm curves for the adsorption of Cu^{2+}, Pb^{2+}, and Cd^{2+} onto PAES-C-Na. [Color figure can be viewed in the online issue, which is available at wileyonlinelibrary.com.]

Na > PAESK-C-Na > PAES. It was known that the factors such as the higher molar ratios of carboxyl and phenylene in the polymers, the stronger ion-exchange and electrostatic attraction between Cu^{2+} and the carboxylic functional groups played an important role in adsorption capacity.[23] It also was noticed that the values of K and n were relatively high for three different materials (Supporting Information Table S1), indicating an increased adsorption capacity and adsorption intensity. Meanwhile, the fact of Langmuir isotherm model that failed to apply in this instance indicated that the adsorption of Cu^{2+} ions was not limited to a simple monolayer mechanism.[1]

Far more significant, further evidence to confirm the adsorption capacity order PAES-C-Na > PAESK-C-Na > PAES was carried out using EDS (Supporting Information Figure S7, ESI), the highest content of Cu^{2+} in the local region of polymeric materials explained that the PAES-C-Na possessed the best adsorption capacity. Simultaneously, the contents of various metal ions in the local region of PAES-C-Na also were identified (Figure 4), which indicated that the adsorption capacity of PAES-C-Na were followed in the order: $Pb^{2+} > Cd^{2+} > Cu^{2+}$, whereas the order was taken in the competitive adsorption: $Pb^{2+} > Cu^{2+} > Cd^{2+}$.

Adsorption Kinetics of Cu^{2+} on PAES-C-Na, PAESK-C-Na, and PAES. In order to investigate the kinetics of metal ion adsorption, two kinetic models were applied[7]: the pseudo-first order model (equation of Lagergreen) [eq. (6)], the pseudo-second order model [eq. (7)]:

$$\log(q_e - q_t) = \log(q_e) - \frac{\kappa_1}{2.303} t \quad (6)$$

$$\frac{t}{q_t} = \frac{1}{\kappa_2 q_e^2} + \frac{t}{q_e} \quad (7)$$

where κ_1 and κ_2 are the pseudo-first order, pseudo-second order adsorption rate constants, respectively, q_e and q_t are the amounts of metal ion adsorbed, per adsorbent mass unit at equilibrium and at time t, respectively.

The results indicated that the pseudo-second-order kinetic model well described the Cu^{2+} adsorption for the PAES-C-Na, PAESK-C-Na, and PAES (Supporting Information Figure S8, Table S2, ESI), based on the correlation coefficients ($R^2 > 0.99$) and the comparison between the calculated equilibrium adsorption capacity ($q_{e,calc}$) and the experimental adsorption capacity ($q_{e,exp}$). Therefore, the rate-limiting step was chemical sorption between the adsorbents and metal ions.[1]

As suggested above, the adsorption capacities of Cu^{2+} were obtained in the order: PAES-C-Na (117.92 mg/g) > PAESK-C-Na (48.9 mg/g) > PAES (26.39 mg/g). Both the high specific area and the precipitates which are easy to be separated due to their settling characteristics also suggested that the PAES-C-Na selected as the optimum adsorbent for the removal of Cu^{2+}, was used to further study the adsorptive properties of Pb^{2+} and Cd^{2+} ions.

Effect of pH on PAES-C-Na

As seen in Figure 5, with the increasing pH values, the adsorbed metal ions onto PAES-C-Na presented the similar phenomenon with the above-mentioned pH effects of Cu^{2+} onto PAES-C-Na. Whereas, the difference in adsorption capacity of different metal ions could be due to the basis of the difference of binding capability between the functional groups onto the surface of adsorbent and metal ions, it tended to be related to charge number of metal ion, charge density onto the adsorbent surface, and extent of metal ion hydrolysis.[33] With regard to hydrolysis and precipitation of the metal ions, an optimal pH of 5.0 was chosen for further studies.

Effect of Contact Time on PAES-C-Na

Figure 6 presented the effect of contact time on Cu^{2+} ions removal. The rate of adsorption increases significantly during a

Table III. Isotherm Parameters for the Adsorption of Cu^{2+}, Pb^{2+}, and Cd^{2+} onto PAES-C-Na

	Linear model		Langmuir model			Freundlich model		
Metal ion	K_d	R^2	q_{max}	b	R^2	n	κ	R^2
Cu^{2+}	0.86	0.9357	47.98	0.2566	0.9686	3.39	15.22	0.9955
Pb^{2+}	1.57	0.8113	69.54	0.7824	0.9837	5.32	35.09	0.9969
Cd^{2+}	1.36	0.8042	64.43	0.3846	0.9926	2.99	20.10	0.9935

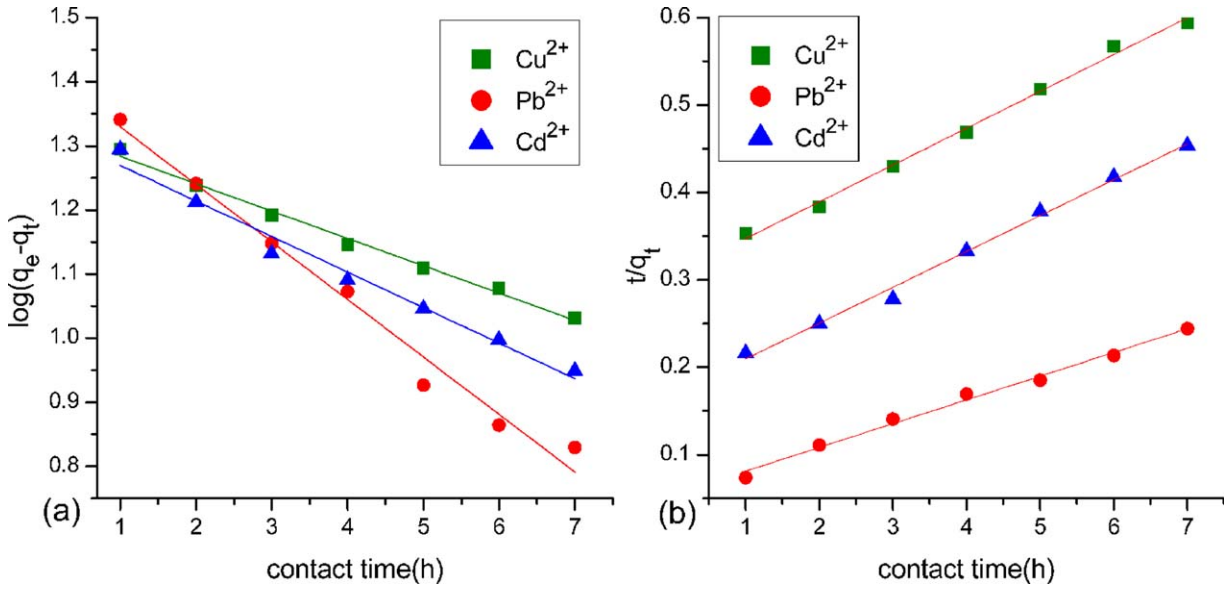

Figure 10. (a) Pseudo-1st-Order and (b) Pseudo-2nd-Order kinetics plots for the adsorption of Cu^{2+}, Pb^{2+}, and Cd^{2+}onto PAES-C-Na. [Color figure can be viewed in the online issue, which is available at wileyonlinelibrary.com.]

first period of about 12 h, and then slowly increases over the all remaining testing period. At higher contact time, the less available surface active sites led to a slight increase of the heavy metal removal capactity.[34]

Effect of Adsorbent Dosage on PAES-C-Na

To fully optimize the reaction conditions, the effects of adsorbent dosage on adsorption of Cu^{2+}, Pb^{2+}, and Cd^{2+} were also investigated. As shown in Figure 7, the adsorption capacities increase progressively with adsorbent dosage. More specially, the increase rate of this parameter was high for higher adsorbent dosages, due to the great availability of active sites on the surface of the PAES-C-Na, and low for lower adsorbent dosages, due to the progressive saturation of these active sites.[1] No significant change was observed as the adsorbent dose was further increased due to the equilibrium status of the concentration of metal ions between the solid and solution phase.

Effect of Initial Concentration on the Polymer PAES-C-Na

Initial metal ion concentration played an important role in the adsorption mechanism investigation.[1] As presented in Figure 8, increasing the initial metal ion concentration resulted in an increase adsorption of Cu^{2+}, Pb^{2+}, and Cd^{2+} per adsorbent mass unit to the equilibrium, which could be interpreted that a higher initial copper ion concentration provided a bigger driving force to overcome mass transfer resistance of the metal ion in a concentration gradient form.[34] Hence a higher initial concentration of metal ion would enhance the adsorption amount of metal ions. However, the removal efficiency of Cu^{2+}, Pb^{2+}, and Cd^{2+} decreased from 87.24% to 23.32%, 97.78% to 35.24% and 92.19% to 30.65%, respectively, as initial metal ion concentration increased, due to the saturation of the active sites on the surface of synthesized polymers.

Adsorption Isotherms of Metal Ions on PAES-C-Na

As seen in Figure 9 and Table III, Freundlich isotherms model (R^2>0.99) fitted much better with the adsorption equilibrium compared with the other models. The reason might be that Freundlich isotherm model based on the assumption of the stronger binding sites were occupied firstly, and the binding strength decreased with an increase in the degree of sorption.[7] The *K* values of Freundlich isotherm model showed that the adsorption capacity increased in the order $Cu^{2+} < Cd^{2+} < Pb^{2+}$ and the *n* values from 1 to 10 indicated favorable adsorption condition, in line with the EDS results aforementioned. On the other hand, Langmuir isotherm model was inferior application in the adsorption of the metal ions onto PAES-C-Na, due to a restrictive monolayer mechanism and the lack of interaction between the adsorbed species. Also, its monolayer maximum adsorption capacity of PAES-C-Na for metal ions followed the order Cu^{2+}

Table IV. Kinetic Parameters for the Adsorption of Cu^{2+}, Pb^{2+}, and Cd^{2+} onto PAES-C-Na

		Pseudo-first-order model			Pseudo-second-order model		
Metal ion	$q_{e,exp}$(mg/g)	$q_{e,calc}$	κ_1	R^2	$q_{e,calc}$	κ_2	R^2
Cu^{2+}	22.53	21.89	0.0982	0.9921	23.75	0.0058	0.9946
Pb^{2+}	35.42	26.25	0.2066	0.9791	36.86	0.0136	0.9907
Cd^{2+}	24.32	21.12	0.1278	0.9771	24.39	0.01	0.9935

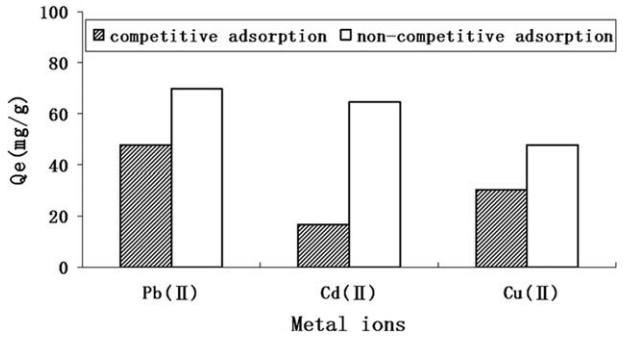

Figure 11. Competitive and noncompetitive adsorption of metal ions onto PAES-C-Na.

(47.98 mg/g) < Cd^{2+} (64.43 mg/g) < Pb^{2+} (69.54 mg/g). It could be found that the adsorption capacity of PAES-C-Na were higher compared with other reported adsorbents, such as chelating resin poly(HEA/MALA) hydrogel (14.5 mg/g of Cu^{2+}, 50.6 mg/g of Cu^{2+}, 20.2 mg/g of Cu^{2+}),[11] and (25.6 mg/g of Cu^{2+}, 38.9 mg/g of Pb^{2+}, 41.3 mg/g of Cd^{2+})[35]. Therefore, PAES-C-Na exhibited a significant potential for metal ions removal.

Adsorption Kinetic of Metal Ions on PAES-C-Na

The fitting curves and results are displayed in Figure 10 and Table IV. It was observed that the pseudo-second-order kinetic model was more suitable to describe the adsorbent systems based on both the correlation coefficients (R^2 > 0.99) and a good agreement between the calculated equilibrium adsorption capacity ($q_{e,calc}$) and the experimental adsorption capacity ($q_{e,exp}$), demonstrating that the rate-limiting step was chemical sorption through sharing the electrons between the adsorbent and metal ions. Similar results have also been reported.[32]

Competitive Adsorption of Metal Ions on PAES-C-Na

The competitive adsorption of the metal ions on PAES-C-Na was investigated in an aqueous solution containing the same concentration (10 mg/L) of Cu^{2+}, Cd^{2+}, and Pb^{2+}. As shown in Figure 11, the adsorption capacities of three metal ions decrease under coexistent condition compared to the respective single-component metal ion adsorption. Under the noncompetitive condition, the competitive adsorption capacities of Pb^{2+} (47.91 mg/g), Cd^{2+} (16.73 mg/g), and Cu^{2+} (30.06 mg/g) were decreased 31.1%, 74.03%, and 37.35%, respectively. And the results also demonstrated that the adsorption of Cd^{2+} ions was significantly affected by the presence of other ions in the solution, Cu^{2+} came secondly, and Pb^{2+} was less impacted. Thus, it could be included that the competitive adsorption of metal ions might be in the order $Pb^{2+} > Cu^{2+} > Cd^{2+}$.

Table V. Adsorption/Desorption Cycle of Cu^{2+}, Pb^{2+}, and Cd^{2+} onto PAES-C-Na

	Cu^{2+}		Pb^{2+}		Cd^{2+}	
Cycle no	*A* (mg/g)	*D* (%)	*A* (mg/g)	*D* (%)	*A* (mg/g)	*D* (%)
1	47.98	87.44	69.54	95.89	64.43	92.12
2	47.19	86.27	68.63	94.64	63.32	90.53
3	46.41	84.58	67.32	92.83	62.72	89.67

A and *D* represent adsorption capacity (mg/g) and desorption percentage (%), respectively.

Regeneration of PAES-C-Na

The reusability of the adsorbents was important for commercial feasibility. The PAES-C-Na samples were investigated after three cycles of consecutive adsorption-desorption procedure and the results were listed in Table V. It elucidated that PAES-C-Na could be used repeatedly without obvious decline of its adsorption capacity, and there were high desorption percentages for all metal ions studied here. After three cycles, the PAES-C-Na (84.58% of Cu^{2+}, 92.83% of Pb^{2+}, 89.67% of Cd^{2+}) with the low cost exhibited the better regeneration capacity, compared to the PEK-L (90.0% of Pb^{2+}, 85.0% of Cd^{2+})[7] and chitosan nanofibril (73.3% of Cu^{2+}, 80.2% of Pb^{2+}, 82.7% of Cd^{2+}).[36]

CONCLUSIONS

In this study, three kinds of high molecular weight of PAES-C, PAESK-C, and PAES, with different molar ratios of carboxyl and phenylene, were successfully synthesized by direct polycondensation in mixture solvent. Compared with PAESK-C-Na and PAES, the PAES-C-Na possessed the largest adsorption capacity of Cu^{2+} and therefore was selected to further explore the adsorption properties of $Pb^{2+}$and Cd^{2+} ions. The adsorption results indicated that the adsorption mechanisms of Pb^{2+}, Cd^{2+}, and Cu^{2+} on PAES-C-Na were due to the combined action of electrostatic interaction and ion-exchange between functional groups and metal ions. The kinetics study revealed that adsorption was more likely modeled by a pseudo-second-order equation. The thermodynamic study illustrated that Freundich model fitted well with the adsorption data. Monolayer adsorption capacity of PAES-C-Na for metal ions was found in the order $Pb^{2+} > Cd^{2+} > Cu^{2+}$. Conversely, the priority order in multi-component adsorption was $Pb^{2+} > Cu^{2+} > Cd^{2+}$. It was also studied that PAES-C-Na was easily regenerated and reused without visible loss of adsorption performance in removing metal ions. These findings suggested that PAES-C-Na was a promising adsorbent to adsorb and recover heavy metal ions from wastewater.

ACKNOWLEDGMENTS

The authors are grateful for the financial support from Liaoning Provincial Department of Education Science general project (L2011079), Liaoning Province Natural Science Fund Project (201202012) and the ministry of Housing and Urban-Rural Development of the People's Republic of China under Grant [2014-K4-034].

REFERENCES

1. Pellera, F. M.; Giannis, A.; Kalderis, D.; Anastasiadou, K.; Stegmann, R.; Wang, J. Y.; Gidarakos, E. *J. Environ. Manage.* **2012**, *96*, 35.
2. Sis, H.; Uysal, T. *Appl. Clay Sci.* **2014**, *95*, 1.
3. Priest, C.; Zhou, J.; Klink, S.; Sedev, R.; Ralston, J. *Chem. Eng. Technol.* **2012**, *35*, 1312.

4. Al-Rashdi, B. A. M.; Johnson, D. J.; Hilal, N. *Desalination* **2013**, *315*, 2.
5. Jacob, K. N.; Kumar, S. S.; Thanigaivelan, A.; Tarun, M.; Mohan, D. *J. Mater Sci.* **2014**, *49*, 114.
6. Feng, T.; Wang, J.; Zhang, F.; Shi, X. W. *J. Appl. Polym. Sci.* **2012**, *128*, 3631.
7. Zhao, X. W.; Zhang, G.; Jia, Q.; Zhao, C. J.; Zhou, W. H.; Li, W. *J. Chem. Eng. J.* **2011**, *171*, 152.
8. He, Q.; Hu, Z.; Jiang, Y.; Chang, X. J.; Tu, Z. F.; Zhang, L. N. *J. Hazard. Mater.* **2010**, *175*, 710.
9. Najafi, M.; Yousefi, Y.; Rafati, A. A. *Curr. Anal. Chem.* **2012**, *85*, 193.
10. Mubarak, N. M.; Sahu, J. N.; Abdullah, E. C.; Jayakumar, N. S. *Sep. Purif. Rev.* **2014**, *43*, 311.
11. Wu, N. M. *Chem. Eng. J.* **2013**, *215-216*, 894.
12. Won, S. W.; Kotte, P.; Wei, W.; Lim, A.; Yun, Y. S. *Bioresour. Technol.* **2014**, *160*, 203.
13. Emik, S. *React. Funct. Polym.* **2014**, *75*, 63.
14. Ahamed, I. S.; Ghonaim, A. K.; Abdel Hakim, A. A.; Moustafa, M. M.; El-Din, K. A. H. *Appl. Sci. Res. J.* **2008**, *4*, 1946.
15. Neagu, V. *J. Hazard. Mater.* **2009**, *171*, 410.
16. Rivas, B. L.; Munoz, C. *J. Appl. Polym. Sci.* **2006**, *101*, 4328.
17. Turkmen, D.; Yılmaz, E.; Oztürk, N.; Akgol, S.; Denizli, A. *Mater. Sci. Eng: C* **2009**, *29*, 2072.
18. Lin, J.; Wang, D. Z.; Liu, L. J.; Zhang, S. Y.; Xu, T. K. *Des. Monomers. Polym.* **2014**, *17*, 425.
19. Zuniga, C.; Larrechi, M. S.; Lligadas, G.; Ronda, J. C.; Galia, M.; Cadiz, V. *J. Polym. Sci. Part A: Polym Chem.* **2011**, *49*, 1912.
20. Zuniga, C.; Lligadas, G.; Ronda, C. J.; Galia, M.; Cadiz, Virginia. *Polymer* **2012**, *53*, 1617.
21. Zhang, Y.; Cui, Z. M.; Zhao, C. J.; Shao, K.; Li, H. T.; Fu, T. Z.; Na, H.; Xing, W. *J. Power Sources* **2009**, *191*, 253.
22. Hendrix, K.; Eynde, M. V.; Koeckelberghs, G.; Vankelecom, I. F. J. *J. Membr. Sci.* **2013**, *447*, 212.
23. Luu, D. X.; Kim, D. *J. Membr. Sci.* **2013**, *430*, 37.
24. Wu, N. M.; Li, Z. K. *Chem. Eng. J.* **2013**, *215*, 894.
25. Liu, D.; Wang, Z. G. *Acta Polym. Sin.* **2010**, *5*, 567.
26. Ma, W. Z.; Zhang, J.; Wang, X. L. *J. Mater. Sci.* **2008**, *43*, 398.
27. Ganesh, S. D.; Harish, M. N. K.; Madhu, B. J.; Maqbool, H.; Pai, K. V.; Kariduraganavar, M. Y. *ISRN Polym. Sci.* **2013**, *2013*, ID: 897034.
28. Kim, J.; Kim, D. *J. Membr. Sci.* **2012**, *405*, 176.
29. Chen, J. H.; Liu, Q. L.; Hu, S. R.; Ni, J. C.; He, Y. S. *Chem. Eng. J.* **2011**, *173*, 511.
30. Krishnan, G. S.; Burkanudeen, A.; Murali, N.; Phadnis, H. *Chinese. J. Polym. Sci.* **2012**, *30*, 664.
31. Hancock, R. D.; Martell, A. E. *Chem. Rev.* **1989**, *89*, 1875.
32. Aksu, Z.; isoglu, I. A. *Process Biochem.* **2005**, *40*, 3031.
33. Li, M.; Li, M. Y.; Feng, C. G.; Zeng, Q. X. *Appl. Surf. Sci.* **2014**, *314*, 1063.
34. Sengil, I. A.; Ozacar, M. *J. Hazard. Mater.* **2009**, *166*, 1488.
35. Tokalioglu, S.; Yilmaz, V.; Kartal, S.; Delibas, A.; Soykan, C. *J. Hazard. Mater.* **2009**, *169*, 593.
36. Liu, D. G.; Li, Z. H.; Zhu, Y.; Li, Z. X.; Kumar, R. *Carbohydr. Polym.* **2014**, *111*, 469.